Contents lists available at ScienceDirect

Computer Physics Communications

www.elsevier.com/locate/cpc

A fast Monte Carlo algorithm for studying bottle-brush polymers

Hsiao-Ping Hsu [a,*], Wolfgang Paul [b]

[a] *Institut für Physik, Johannes Gutenberg-Universität Mainz, Staudinger Weg 7, 55099 Mainz, Germany*
[b] *Theoretische Physik, Martin Luther Universität Halle-Wittenberg, von Seckendorff Platz 1, 06120 Halle, Germany*

ARTICLE INFO

ABSTRACT

Obtaining reliable estimates of the statistical properties of complex macromolecules by computer simulation is a task that requires high computational effort as well as the development of highly efficient simulation algorithms. We present here an algorithm combining local moves, the pivot algorithm, and an adjustable simulation lattice box for simulating dilute systems of bottle-brush polymers with a flexible backbone and flexible side chains under good solvent conditions. Applying this algorithm to the bond fluctuation model, very precise estimates of the mean square end-to-end distances and gyration radii of the backbone and side chains are obtained, and the conformational properties of such a complex macromolecule are studied. Varying the backbone length (from $N_b = 67$ to $N_b = 1027$), side chain length (from $N = 0$ to $N = 24$ or 48), the scaling predictions for the backbone behavior as well as the side chain behavior are checked. We are also able to give a direct comparison of the structure factor between experimental data and the simulation results.

1. Introduction

The so-called "bottle-brush polymers" consist of a long macromolecule serving as a "backbone" on which many flexible side chains are densely grafted [1–4]. In nature, bottle-brushes like aggrecans have been found in the cartilage of mammalian including human joints and are held responsible for the excellent lubrication properties in such joints [5,6]. Recently, the chemical synthesis of such complex molecular bottle-brushes has become possible in laboratories with newly developed synthetic techniques [7–10]. Theoretical predictions [11–42] of the conformational properties of bottle-brush polymers based on the blob picture, the scaling theory, and the self-consistent field theory have also been worked out. However, in order to check the theoretical predictions and to give a reasonable explanation for the experimental results or to control the functions of bottle-brush polymers computer simulations are needed for a deeper understanding of the structure of these macromolecules.

"Static" Monte Carlo (MC) algorithms (simple sampling of self-avoiding walks (SAWs)), extensions such as dimerization, enrichment techniques, Rosenbluth's inversely restricted sampling and the pruned enriched Rosenbluth method (PERM) do not converge for very large branched polymers such as bottle-brushes. "Dynamic" MC algorithms also encounter serious problems, since the relaxation times of these polymers are expected to be excessively large, and hence prohibitively long MC simulations would

be required. In the early work on bottle-brush polymers in a good solvent, both lattice and off-lattice models were used for MC simulations. Using the bond fluctuation model [43–46] on a simple cubic lattice, applying local moves to the bottle-brush polymers, side chain lengths up to $N = 64$, backbone lengths up to $N_b = 64$, and grafting densities up to $\sigma = 1$ were studied in [26]. In combination with the pivot move algorithm, N_b up to 800, N up to 80, and $\sigma < 1/3$ were studied in [22,25]. Using flexible freely jointed chains [23,32] and the bead-spring model [35] with hard sphere interactions in a continuous space and using the pivot moves, the largest bottle-brush polymers which were studied were $N_b = 402$, $N = 25$, and $\sigma = 1$, and using the Metropolis algorithm for the latter model, maximum values of $N_b = 100$, $N = 50$ were studied. However, although all these studies are very interesting and stimulating, the accessible parameter range clearly was not large enough (and the accuracy of the results not precise enough) to allow a straightforward test of the theoretical concepts, and thus a need for further work with different methods clearly did emerge.

In our previous work [37,38], we were able to simulate bottle-brush polymers with rigid linear backbone and flexible side chains under various solvent conditions by applying a variant of the PERM algorithm [47] to a simple lattice model with periodic boundary conditions along the backbone. Under good solvent conditions, we have shown that the power laws predicted for the side chain behavior are still difficult to reach although the maximum side chain length in our simulation was $N = 2000$. However, a crossover behavior from 3D SAW-like side chains to stretched side chains was presented in [37,38] as the side chain length or the grafting density increased. Of course, removing all configurational degrees of freedom of the backbone was a crucial prerequisite to allow the

(a) (b)
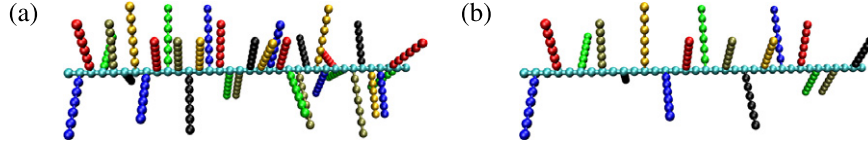
Fig. 1. Snapshots of initial configurations of bottle-brush polymers with $N_b = 35$ monomers on the backbone and $N = 6$ monomers on each side chain, showing the geometry of our model for bottle-brush polymers with the grafting densities (a) $\sigma = 1$ and (b) $\sigma = 1/2$.

successful use of the PERM algorithm, but it also means that highly interesting questions (such as backbone stiffening due to the side chains) could not be studied.

Recently, we have focused on the comparison of structure factors to experimental data and on the persistence length [40–42] of the backbone using the bond fluctuation model on a simple cubic lattice. This communication will discuss in detail the algorithm we developed for these simulations. It is introduced in Section 2, and results for the conformational properties of bottle-brush polymers only achievable by this very efficient simulation approach are shown in Section 3. Finally, our conclusions are presented in Section 4.

2. Model and simulation methods

For studying bottle-brush polymers with a flexible backbone and with flexible side chains under very good solvent conditions so that only excluded volume effects are considered, we generalize the standard bond fluctuation model for linear polymers [43–46] to bottle-brush polymers. In the standard bond fluctuation model, a flexible polymer chain with excluded volume interactions is described by a chain of effective monomers on a simple cubic lattice (the lattice spacing is the unit of length). Each effective monomer blocks all 8 corners of an elementary cube of the lattice from further occupation. Two successive monomers along a chain are connected by a bond vector $\vec{b}$ which is taken from the set $\{(\pm 2, 0, 0), (\pm 2, \pm 1, 0), (\pm 2, \pm 1, \pm 1), (\pm 2, \pm 2, \pm 1), (\pm 3, 0, 0), (\pm 3, \pm 1, 0)\}$, including also all permutations. The bond length $|\vec{b}| = \ell_b$ is in a range between 2 and $\sqrt{10}$. There are in total 108 bond vectors serving as candidates for building the conformational structure of bottle-brush polymers.

As shown in Fig. 1, the geometry of the bottle-brush polymer is arranged in a way that side chains of length N are added to the backbone at a regular spacing $1/\sigma$ (σ is the grafting density), and two additional monomers are added to the two ends of the backbone. Thus, the number of monomers of the backbone N_b is related to the number of side chains n_c via

$$N_b = \left[(n_c - 1)/\sigma + 1 \right] + 2, \qquad (1)$$

and the total number of monomers of the bottle-brush polymer is $N_{tot} = N_b + n_c N$. Creating an initial configuration of a bottle-brush polymer that does not violate any excluded volume constraint would be a highly nontrivial matter if we would require that both backbone and side chains are already coiled. Thus one simple way to construct an initial configuration of bottle-brush polymers in the simulation is to assume that the backbone and all side chains are rigid rod-like structures. In order to fit the criteria of the bond fluctuation model without further checking, the backbone is placed in the direction along the z-axis with fixed bond length $\ell_b = 3$ between two successive monomers on the backbone. The bond vectors of each side chain are chosen randomly from one of the allowed bond vectors in the (xy)-plane, but the bond vectors used to connect the monomers on the same side chain starting from the grafting site on the backbone are the same.

In our algorithm, instead of trying to move a monomer to the nearest neighbor sites in the six directions ("L6" move), $\pm \hat{x}$, $\pm \hat{y}$,

and $\pm \hat{z}$ for the standard bond fluctuation model, we use the local 26 ("L26") moves [48]. Namely, the chosen monomer is allowed to move to not only the nearest neighbor sites but also the next neighbor sites, and the sites at the 8 corners, which are located $\sqrt{2}$, and $\sqrt{3}$ lattice spacings away from the chosen monomer, respectively. The move is accepted only if the selected new positions are empty and the bond length constraints are satisfied. The key point of this move is that it allows for crossings of bonds during the move; no such simple moves that allow bond crossing for the simple SAW model (where the bond length is fixed to one lattice spacing) are known. Without the possibility of bond crossing, two side chains of the bottle-brush that happen to be entangled with each other would relax this topological constraint only extremely slowly.

Since neighboring side chains are rigidly grafted to neighboring "anchor points" at the backbone, they can never diffuse away from each other, unlike free chains in a solution or melt; thus topological constraints could relax only via an "arm retraction mechanism" familiar from star polymers, if the algorithm ensures non-crossability of chains. This arm retraction leads to an extremely long relaxation time. This problem is avoided by the "L26" moves. Applying the "L26" move algorithm to a small bottle-brush polymer of 431 monomers ($N_b = 35$, $N = 12$, and $\sigma = 1$), results of the time series of the square gyration radius of the backbone scaled with the scaling law for 3D SAWs, $R_{gb}^2(t)/N^{2\nu}$ ($\nu = 0.588$), and the time series of the shape change of bottle-brush polymers, which is described by the space occupation in the Cartesian coordinates $(\Delta_x(t), \Delta_y(t), \Delta_z(t))$ shown in Fig. 2 indicate that it needs about 10^6 MC steps to reach an equilibrium state. Here one MC step is a sequence of N_{tot} "L26" moves (each monomer is attempted to move once). As the number of monomers on the backbone increases to $N_b = 515$, i.e., the total number of monomers increases to $N_{tot} = 6671$, one would expect for a Rouse scaling of the relaxation time $\tau \sim N^{1+2\nu}$ that it might need about 400 times the number of MC steps to reach an equilibrium state. Unfortunately, the simple Rouse behavior does not describe the scaling of the relaxation time for the bottle-brushes and the relaxation time increases even faster as shown in the inset of Fig. 3.

In our simulations, the lattice size $V = L_x \times L_y \times L_z$ is chosen large enough so that no monomer can interact with itself. The ith monomer located at the site $\vec{r}_i = (x_i, y_i, z_i)$ is denoted by $p_i = z_i + y_i L_z + x_i L_y L_z$. No periodic boundary condition is considered here but a hashing method is used to map the position of monomers back into the original box. For small bottle-brush polymers it is possible to set the lengths of the simple cubic lattice equal in each dimension, i.e., $L_x = L_y = L_z = 3N_b$ (the maximum length determined by the initial configuration), while for large bottle-brush polymers one encounters difficulties in the limitation of computer memory. Therefore, in order to be able to simulate large bottle-brush polymers, a new method is introduced which separates the equilibrating process into several stages. The maximum lattice size which we can use on the computer is 2^{28}. Thus, we first choose $L_z = 3N_b$, $L_y = L_x$, and $V = L_z L_y L_x \leqslant 2^{28}$. As shown in Fig. 3, the time series of $\Delta_x(t)$, $\Delta_y(t)$, and $\Delta_z(t)$ as well as configurations in the intermediate state are stored. After t_f MC steps, we reset the size of the lattice by decreasing L_z to $L_z = \Delta_z(t_f)$ but increasing L_y and L_x to $L_y = L_x = \text{Integer}\{(2^{28}/\Delta_z(t_f))^{1/2}\} \geqslant$
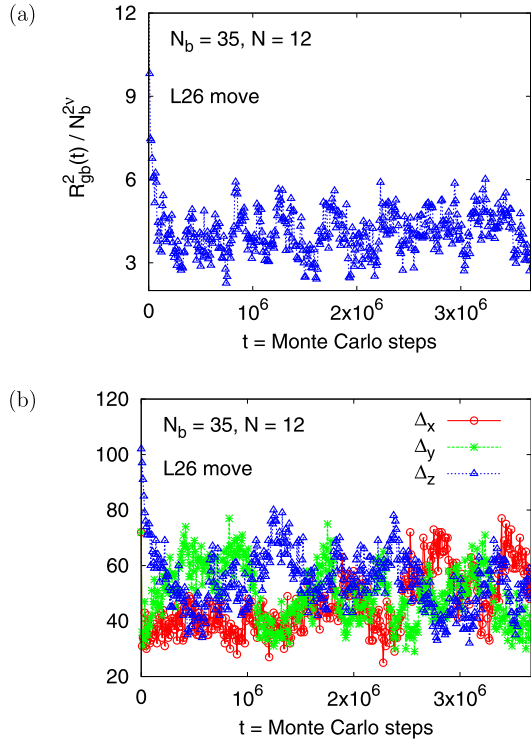
Fig. 2. Time series of the rescaled square gyration radii for the backbone monomers, $R_{gb}^2(t)/N^{2\nu}$ (a), and the space occupations in the Cartesian coordinates $(\Delta_x(t), \Delta_y(t), \Delta_z(t))$ (b). Here we apply the "L26" move algorithm to simulate the bottle-brush polymers of $N_b = 35$, $N = 12$, and $\sigma = 1$.
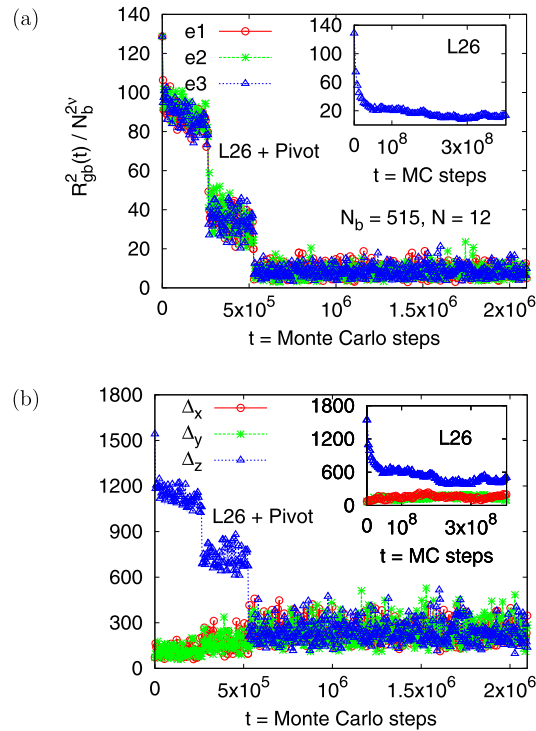
Fig. 3. Time series of the rescaled square gyration radii for the backbone monomers, $R_{gb}^2(t)/N_b^{2\nu}$ (a), and the space occupations in the Cartesian coordinates $(\Delta_x(t), \Delta_y(t), \Delta_z(t))$ (b). Here we apply the "L26 + pivot" algorithm to simulate a bottle-brush polymer of $N_b = 515$, $N = 12$, and $\sigma = 1$. The time series obtained when using the "L26" move is shown in the inset. The legends e1, e2, e3 in (a) indicate three different starting configurations.

$\max(\Delta_y(t_f), \Delta_x(t_f))$. Here t_f is the number of MC steps at the current stage, which can be adopted to the simulation such that the conditions $\Delta_x < L_x$ and $\Delta_y < L_y$ hold. We repeat the same procedure until $L_x = L_y = L_z$ since the space occupation of the conformations of bottle-brush polymers must be isotropic.

To speed up the equilibrating process and the time for generating independent configurations, in addition to the local "L26" move [48] also pivot moves [49] are used. Two types of moves are attempted (see Fig. 4):

(i) A monomer on the backbone is chosen randomly and the short part of the bottle-brush polymer is transformed by randomly applying one of the 48 symmetry operations (no change; rotations by 90° and 180°; reflections and inversions) to the adjacent bond.

(ii) A monomer is chosen randomly from all the side chain monomers, and the part of the side chain from the selected monomer to the free end of the side chain is transformed by one of the 48 symmetry operations.

Again, we apply the "L26 + pivot" algorithm to the bottle-brush polymers with $N_b = 515$, $N = 12$, and $\sigma = 1$ but start the simulations from three different initial configurations named by e1, e2, and e3. From the results shown in Fig. 3, we see that the equilibrium states are reached in less than 10^6 MC steps. Here one MC step is a sequence of N_{tot} "L26" moves, k_{pb} pivot moves of the backbone and k_{pc} pivot moves of side chains; k_{pb} is chosen such that the acceptance ratio is about 40% or even larger, while $k_{pc} = n_c/4$. It takes about 1.25 hours CPU time on an Intel 2.80 GHz PC to reach the equilibrium state (after 10^6 MC steps are performed) for one single simulation of bottle-brush polymers ($N_b = 515$, $N = 12$, and $\sigma = 1$) with $N_{tot} = 6671$, $k_{pb} = 40$, and $k_{pc} = 128$.

Another important point one has to be aware of is that the monomers on the backbone, labeled as $0, 1, \ldots, N_b - 1$, which can be selected as a pivot point for applying the pivot move are also limited due to the size of the lattice we set up before reaching the equilibrium state. However, once the system is in equilibrium one has to allow all possible moves ($1 \leqslant N_b^p \leqslant (N_b - 2)$) with the "L26 + pivot" algorithm. For the case shown in Fig. 3, the equilibrating process is divided into four stages:

stage 1: $1 \leqslant N_b^p \leqslant 128$, $L_z = 1545$, $L_y = L_x = 415$, $t_f = 262\,144$ MC steps,

stage 2: $1 \leqslant N_b^p \leqslant 256$, $L_z = 1201$, $L_y = L_x = 473$, $t_f = 262\,144$ MC steps,

stage 3: $1 \leqslant N_b^p \leqslant 513$, $L_z = 851$, $L_y = L_x = 561$, $t_f = 262\,144$ MC steps,

stage 4: $1 \leqslant N_b^p \leqslant 513$, $L_z = L_y = L_x = 645$, $t_f = 1\,310\,720$ MC steps.

As a caveat, the number of stages needed for the system reaching the equilibrium is empirical. It varies according to the size of the backbone length and fluctuations from one equilibration path to the other equilibration path. When one simulates an end-grafted bottle-brush polymer adsorbed to an impenetrable flat surface, it also varies depending on the attractive interactions between the monomers and the surface. Due to the fluctuation of the conformations of bottle-brush polymers, the time series of the square gyration radius of the backbone, $R_{gb}^2(t)$, and the space occupations in the Cartesian coordinates $(\Delta_x(t), \Delta_y(t), \Delta_z(t))$ of the bottle-brush polymers (similar to the functions shown in Fig. 3) are required in order to determine the lengths of the simulation box for the next stage and to check whether the equilibrating process is finished or not.
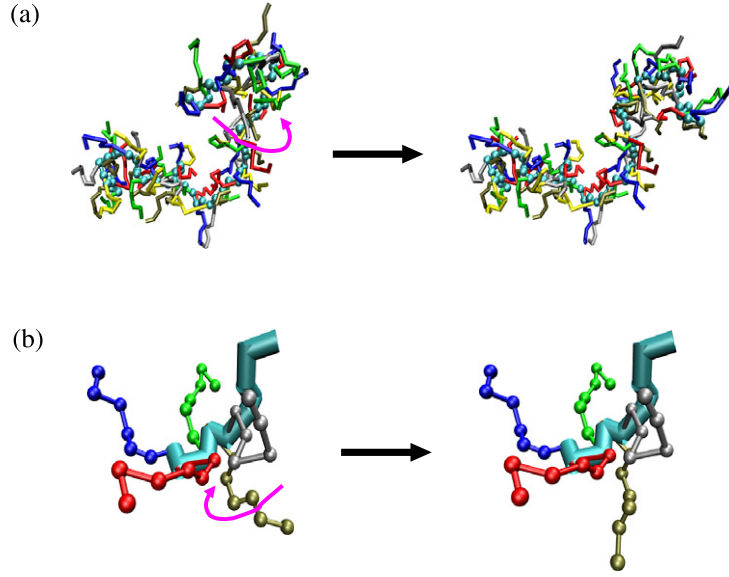
Fig. 4. Pivot moves applied to a randomly chosen monomer on the backbone (a) and on one of the side chains (b).
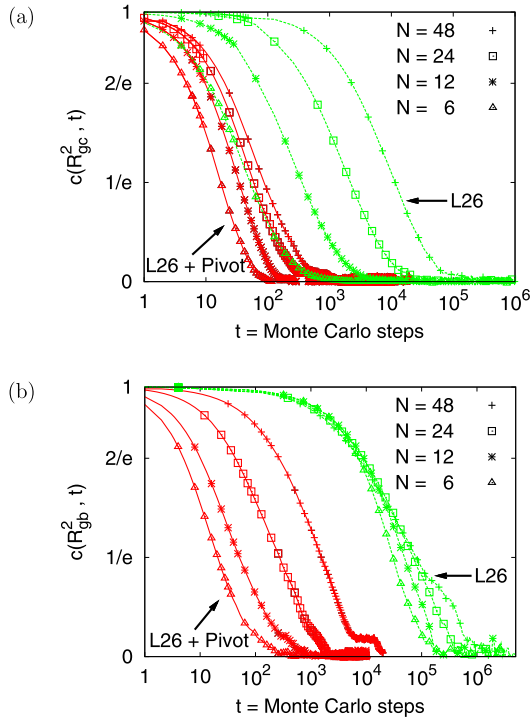
Fig. 5. Autocorrelation functions of the mean square gyration radii for the side chains $c(R_{gc}^2, t)$ (taking the average of all side chains at t) (a), and for the backbone $c(R_{gb}^2, t)$ (b), plotted vs. the number of Monte Carlo steps t. Data obtained for bottle-brush polymers with backbone length $N_b = 35$, side chain lengths $N = 48$, 24, 12, and 6, and grafting density $\sigma = 1$ when using the "L26" moves and the "L26 + pivot" moves are shown by the dashed and solid curves, respectively.

The efficiency of the algorithm and the number of MC steps needed for getting an independent configuration for the measurement were determined by the autocorrelation function $c(A, t)$,

$$c(A, t) = \frac{\langle A(t_0) A(t_0 + t) \rangle - \langle A(t_0) \rangle \langle A(t_0 + t) \rangle}{\langle A(t_0)^2 \rangle - \langle A(t_0) \rangle^2}, \qquad (2)$$

where A is an observable. Results of $c(A, t)$ for the mean square gyration radius of the backbone, $A = R_{gb}^2$, and of the side chains, $A = R_{gc}^2$ (taking the average of all side chains at the same Monte

Carlo time t) plotted against the number of MC steps t are shown in Fig. 5 for $N_b = 35$. We see that the "L26 + pivot" algorithm is two orders of magnitude faster than the "L26" algorithm for the four cases of bottle-brush polymers (backbone length $N_b = 35$, grafting density $\sigma = 1$, and side chain lengths $N = 48, 24, 12$, and 6) we chose. Also, increasing the side chain length from $N = 6$ to $N = 48$, the autocorrelation time for the side chain structural relaxation increases by more than two orders of magnitude for the "L26" case and by less than one order of magnitude for the "L26 + pivot" case. When we increase the backbone length N_b to $N_b = 515$ and adjust the number of pivot moves for the side chains tried from $k_{pc} = 8$ to $k_{pc} = 128$ in each Monte Carlo step such that on average about 1/4 of the side chains is tried for a pivot move in each MC step, we can see in part (a) of Fig. 6 that the decay of the autocorrelation function for the side chain structure occurs on the same time scale, i.e., it is only the average number of pivot moves per side chain which determines the autocorrelation time. The same is true for the backbone as we can see in part (b) of that figure. Here we plot the autocorrelation function explicitly against the total number of pivot moves tried, tk_{pb}, and it is obvious that the structural relaxation for the much longer backbone chain occurs on the same time scale as the one for the short backbone chain. A systematic increase of the relaxation time for both, side chains and backbone, as a function of side chain length remains, however. The stage wise decomposition of the equilibrating process, with the appropriate adjustment of the simulation volume, as described above, is a crucial step of our procedures, and a novel ingredient, not used in other contexts, and was a prerequisite for successful simulations.

3. Results

In order to test our program, we first simulated linear polymer chains of N_b monomers under good solvent conditions, i.e., $N = 0$. According to the scaling law of the mean square end-to-end distance, R_{eb}^2, one should expect that the curve of $\langle R_{eb}^2 \rangle / N_b^{2\nu}$ becomes horizontal as $N_b \to \infty$. Here $\nu = 0.588$ is the Flory exponent for the 3D SAW. This is indeed seen in Fig. 7. Using the "L26 + pivot" algorithm, we can simulate bottle-brush polymers with a number of monomers on the backbone up to $N_b = 1027$, side chain length up to $N = 24$ for $N_b > 259$, and side chain length up to $N = 48$ for $N_b \leqslant 259$. The results shown in Fig. 7 are the average of 10^5–10^6
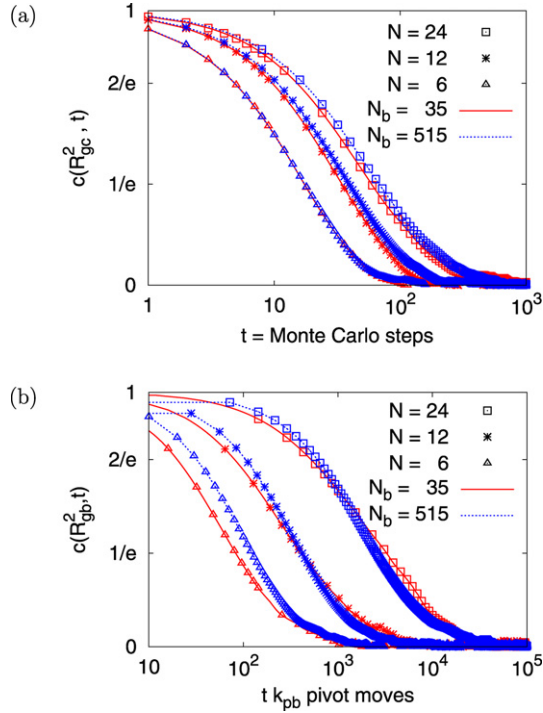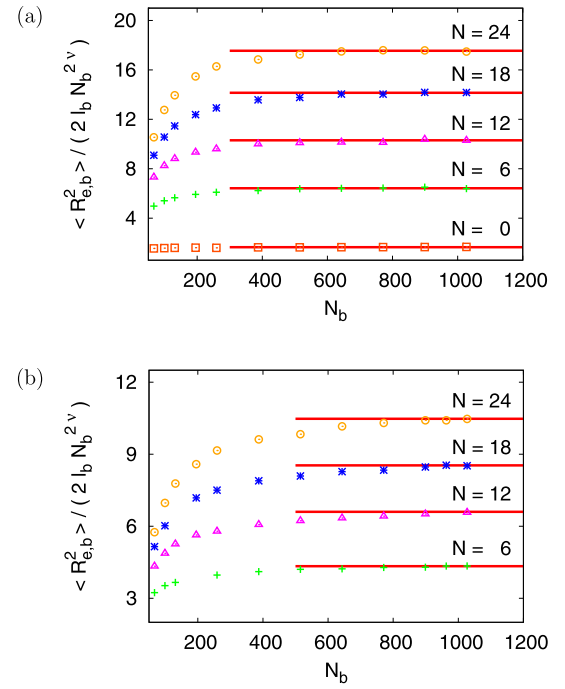
Fig. 6. (a) Autocorrelation function of the mean square gyration radii for the side chains $c(R_{gc}^2, t)$ as a function of Monte Carlo time t. Both for $N_b = 35$ and $N_b = 515$, one pivot move per side chain is tried on average every 4 MC steps. (b) Autocorrelation function for the backbone $c(R_{gb}^2, t)$ plotted vs. the total number of pivot moves done, comparing the relaxation for $N_b = 35$ and for $N_b = 515$.

Fig. 7. Rescaled mean square end-to-end distance $\langle R_{eb}^2 \rangle/(2\ell_b N_b^{2\nu})$ ($\nu = 0.588$) plotted against backbone length N_b for bottle-brush polymers with grafting density $\sigma = 1$ (a) and $\sigma = 1/2$ (b). Various values of side chain length N are shown ($N = 0$ means that no side chains are grafted at all). Horizontal straight lines indicate the estimates for the persistence length, $\ell_{p,R}$.

independent configurations. The error bars are given by the standard deviations of the average, which are smaller than the size of symbols. Increasing the side chain length N, but keeping the grafting density fixed to $\sigma = 1$ or $\sigma = 1/2$, one observes an increase in $\langle R_{eb}^2 \rangle/N_b^{2\nu}$ for a fixed value of N_b, which shows that the stretching of the backbone is induced by the chain length N as well as the grafting density σ, whereas one observes that the backbone of the bottle-brush polymers behaves like a SAW with increasing N_b but fixed N. In Refs. [41,42], it has been pointed out that the persistence length $\ell_{p,R}$ which describes the intrinsic stiffness of bottle-brush polymers can be determined by the mean square end-to-end distance of the backbone, R_{eb}^2,

$$\langle R_{eb}^2 \rangle = 2\ell_{p,R}\ell_b N_b^{2\nu}. \tag{3}$$

Here $\ell_b \approx 2.7$ is the average bond length of polymer chains for the bond fluctuation model. The snapshots of conformations of bottle-brush polymers which contain 131 monomers on the backbone and N monomers on each side chain in a good solvent displayed in Fig. 8 also show that the backbone becomes stiffer as the side chain length N increases from 6 to 48.

Another quantity which can be used to examine whether the system does reach the equilibrium and the statistics are reliable enough is the mean square end-to-end distance $\langle R_{ec,\perp}^2 \rangle$ (or radius of gyration $\langle R_{gc,\perp}^2 \rangle$) of the side chains along the backbone in the direction perpendicular to the backbone. For bottle-brush polymers of a flexible backbone, the perpendicular direction is determined by the vector pointing from the grafting site to the center of mass of the corresponding grafted side chain. Plotting $\langle R_{ec,\perp}^2 \rangle/N^{2\nu}$ against the normalized position $k/(n_c - 1)$ for $k = 0, 1, \ldots, n_c - 1$ in Fig. 9, a plateau appears with tiny fluctuations for $0.2 < k < 0.8$ showing that in the interior of bottle-brush polymers the side chains behave the same for fixed side chain lengths N as expected after taking the average over sufficiently many independent samples. The side chains stretch away more from the backbone as the

side chain length N and the grafting density σ increases. The decreasing behavior of $\langle R_{ec,\perp}^2 \rangle$ for the side chains near the two ends of the backbone obviously arises from the fact that monomers on these side chains have more freedom to move.

Finally, a comparison of the structure factor $S(q)$ between the experimental data [9] and our simulation results [41] is shown in Fig. 10. The normalized structure factor $S(q)$ is defined by

$$S(q) = \frac{1}{N_{\text{tot}}^2} \sum_{i=1}^{N_{\text{tot}}} \sum_{j=1}^{N_{\text{tot}}} \langle c(\vec{r}_i)c(\vec{r}_j) \rangle \frac{\sin(q|\vec{r}_i - \vec{r}_j|)}{q|\vec{r}_i - \vec{r}_j|}, \tag{4}$$

where $c(\vec{r}_i)$ is an occupation variable, $c(\vec{r}_i) = 1$ if the site $\vec{r}_i$ is occupied by a bead, and zero otherwise. Note that an angular average over the direction of the scattering vector $\vec{q}$ has been performed, and the sums run over all monomers (all side chains and the backbone). Adjusting only the number of monomers on the backbone, N_b, and the number of monomers on each side chain, N, the results for the bottle-brush polymers of $N_b = 259$, $N = 48$, and $\sigma = 1$ are mapped to the data for the experimental sample of $N_b^{\text{exp}} = 400$, $N^{\text{exp}} = 62$ and $\sigma^{\text{exp}} \approx 1$ when the momentum q is scaled by R_g. Here R_g is the gyration radius of the whole bottle-brush polymer. In this case, $R_g = 115.8$ (lattice spacings) is obtained from our MC simulations and $R_g = 30.5$ nm is obtained from the experimental data. One can immediately translate 1 nm ≈ 3.79 lattice spacing. Clearly, translating the length units from the large-scale structure (small q behavior) and choosing the length of backbone and side chains correctly, one obtains a faithful description of the experimental scattering function over the whole q-range studied.

4. Conclusion

We have presented extensive MC simulations for bottle-brush polymers under good solvent conditions using the bond fluctuation model with a newly developed efficient MC algorithm combining the "L26" moves, the pivot moves, and an adjustable simulation
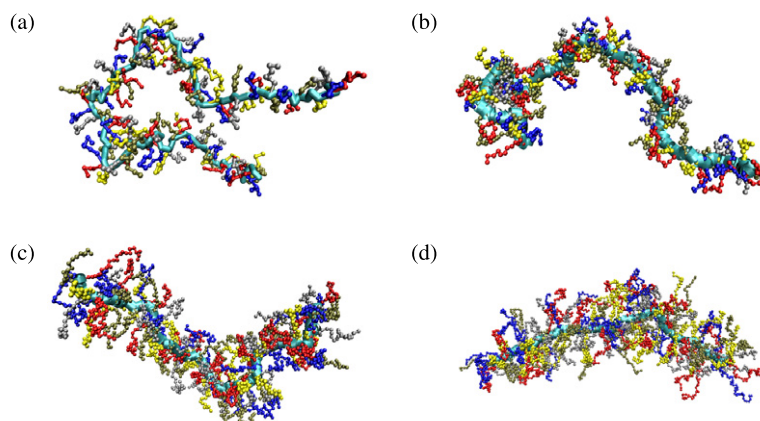
Fig. 8. Snapshots of the conformations of bottle-brush polymers with $N_b = 131$ monomers on the backbone and with side chain lengths (a) $N = 6$, (b) $N = 12$, (c) $N = 24$, and (d) $N = 48$.
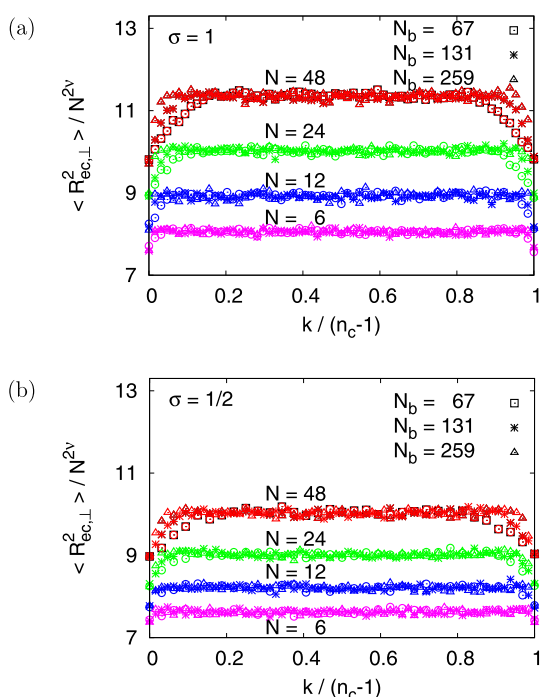
Fig. 9. Rescaled mean square end-to-end distance of the side chains in perpendicular direction $\langle R_{ec,\perp}^2 \rangle / N^{2\nu}$ ($\nu = 0.588$), plotted vs. the normalized position $k/(n_c - 1)$ in the coordinate system along the backbone (the n_c side chains are labeled by $k = 0, 1, \ldots, n_c - 1$). Four choices of side chain length $N = 6, 12, 24$, and 48, and three choices of backbone length $N_b = 67, 131$, and 259 are included, as indicated. Case (a) refers to $\sigma = 1$, and case (b) to $\sigma = 1/2$.

lattice box which changes its shape from a very elongated parallelepiped to a cube as the equilibration of the bottle-brush polymer conformation from an initial stretched backbone to a coiled conformation proceeds. Using this fast algorithm to generate a sufficiently large number of independent configurations in equilibrium, we are able to obtain high accuracy estimates of the related characteristic length scales for describing the conformational properties of bottle-brush polymers, such as the end-to-end distance of a side chain and the backbone, the persistence length of the backbone, the effective cross-sectional radius of the whole bottle-brush polymers, etc. From the computer simulations, the scattering intensity contributed by any part of the bottle-brush polymers is calculated directly. Therefore, we are also able to compare our simulation result to the experimental data directly and test those models used in the analysis of experimental data.
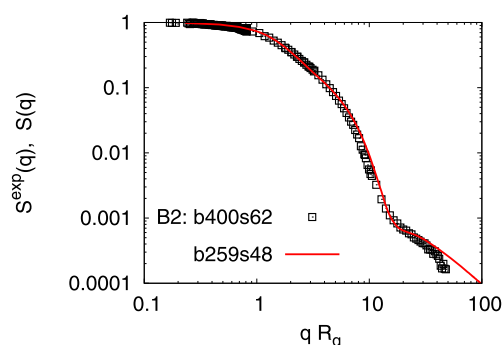
Fig. 10. Normalized structure factor $S^{exp}(q)$ plotted vs. qR_g for the sample with $N_b^{exp} = 400$, $N^{exp} = 22$ [9], compared with simulated structure factor $S(q)$ for $N_b = 259$, $N = 48$ [41]. $R_g = 30.5$ nm obtained from the experimental data [9] and $R_g = 115.8$ (lattice spacing) from the simulation result [41].

Recently, this algorithm has also been employed successfully to study the conformational change of bottle-brush polymers as they are absorbed on a flat solid surface by varying the attractive interaction between the monomers and the surface [50]. In our future work, it will be interesting to see how far this algorithm can be applied for studying bottle-brush polymers under poorer solvent conditions.

Acknowledgements

References

[1] M. Zhang, A.H.E. Müller, Cylindrical polymer brushes, J. Polym. Sci. Part A, Polymer Chemistry 43 (2005) 3461–3481.
[2] A.V. Subbotin, A.N. Semenov, Spatial self-organization of comb macromolecules, Polym. Sci. Ser. A 49 (2007) 1328–1357.
[3] S.S. Sheiko, B.S. Sumerlin, K. Matyjaszewski, Cylindrical molecular brushes: Synthesis, characterization, and properties, Prog. Polym. Sci. 33 (2008) 759–785.
[4] I.I. Potemkin, V.V. Palyulin, Comblike macromolecules, Prog. Polym. Sci. 51 (2009) 123–149.

[5] J. Klein, Molecular mechanisms of synovial joint lubrication, Proc. Inst. Mech. Eng. Part J 220 (2006) 691–710.

[6] J. Klein, Repair or replacement – A joint perspective, Science 323 (2009) 47–48.

[7] M. Wintermantel, M. Schmidt, Y. Tsukahara, K. Kajiwara, S. Kohjiya, Rodlike combs, Macromol. Chem. Rapid. Commun. 15 (1994) 279–284.

[8] M. Wintermantel, M. Gerle, K. Fischer, M. Schmidt, I. Wataoka, H. Urakawa, K. Kajiwara, Y. Tsukahara, Molecular bottlebrushes, Macromolecules 29 (1996) 978–983.

[9] S. Rathgeber, T. Pakula, K. Matyjaszewski, K.L. Beers, On the shape of bottle-brush macromolecules: Systematic variation of architectural parameters, J. Chem. Phys. 122 (2005) 124904, 13 pp.

[10] B. Zhang, F. Gröhn, J.S. Pedersen, K. Fischer, M. Schmidt, Conformation of cylindrical brushes in solution: Effect of side chain length, Macromolecules 39 (2006) 8440.

[11] T.M. Birshtein, E.B. Zhulina, Conformations of star-branched macromolecules, Polymer 25 (1984) 1453–1461.

[12] T.A. Witten, P.A. Pincus, Colloid stabilization by long grafted polymers, Macromolecules 19 (1986) 2509–2513.

[13] T.M. Birshtein, O.V. Borisov, Ye.B. Zhulina, A.R. Khokhlov, T.A. Yurasova, Conformations of comb-like macromolecules, Polym. Sci. USSR 29 (1987) 1293–1300.

[14] Z.-G. Wang, S.A. Safran, Size distribution for aggregates of associating polymers. II. Linear packing, J. Chem. Phys. 89 (1988) 5323–5328.

[15] C. Ligoure, L. Leibler, Decoration of rough surfaces by chain grafting, Macromolecules 23 (1990) 5044–5046.

[16] R.C. Ball, J.F. Marko, S.T. Milner, T.A. Witten, Polymers grafted to a convex surface, Macromolecules 24 (1991) 693–703.

[17] M. Murat, G.S. Grest, Polymers end-grafted onto a cylindrical surface, Macromolecules 24 (1991) 704–708.

[18] N. Dan, M. Tirrell, Polymers tethered to curved interfaces. A self-consistent-field analysis, Macromolecules 25 (1992) 2890–2895.

[19] G.H. Fredrickson, Surfactant-induced lyotropic behavior of flexible polymer solutions, Macromolecules 26 (1993) 2825–2831.

[20] E.B. Zhulina, T.A. Vilgis, Scaling theory of planar brushes formed by branched polymers, Macromolecules 28 (1995) 1008–1015.

[21] E.M. Sevick, Shear swelling of polymer brushes grafted onto convex and concave surface, Macromolecules 29 (1996) 6952–6958.

[22] Y. Rouault, O.V. Borisov, Comb-branched polymers: Monte Carlo simulation and scaling, Macromolecules 29 (1996) 2605–2611.

[23] M. Saariaho, O. Ikkala, I. Szleifer, I. Erukhimovich, G. ten Brinke, On lyotropic behavior of molecular bottle-brushes: A Monte Carlo computer simulation study, J. Chem. Phys. 107 (1997) 3267–3276.

[24] M. Saariaho, I. Szleifer, O. Ikkala, O.G. ten Brinke, Extended conformations of isolated molecular bottle-brushes: Influence of side-chain topology, Macromol. Theory Simul. 7 (1998) 211–216.

[25] Y. Rouault, From comb polymers to polysoaps: A Monte Carlo attempt, Macromol. Theory Simul. 7 (1998) 359–365.

[26] K. Shiokawa, K. Itoh, N. Nemoto, Simulations of the shape of a regularly branched polymer as a model of a polymacromonomer, J. Chem. Phys. 111 (1999) 8165–8173.

[27] M. Saariaho, A. Subbotin, I. Szleifer, O. Ikkala, G. ten Brinke, Effect of side chain rigidity on the elasticity of comb copolymer cylindrical brushes: A Monte Carlo simulation study, Macromolecules 32 (1999) 4439–4443.

[28] A. Subbotin, M. Saariaho, O. Ikkala, G. ten Brinke, Elasticity of comb copolymer cylindrical brushes, Macromolecules 33 (2000) 3447–3452.

[29] M. Saariaho, A. Subbotin, O. Ikkala, G. ten Brinke, Comb copolymer cylindrical brushes containing semiflexible side chains: a Monte Carlo study, Macromol. Rapid. Commun. 21 (2000) 110–115.

[30] P.G. Khalatur, D.G. Shirvanyanz, N.Y. Starovoitova, A.R. Khokhlov, Conformational properties and dynamics of molecular bottle-brushes: A cellular-automaton-based simulation, Macromol. Theory Simul. 9 (2000) 141–155.

[31] V.V. Vasilevskaya, A.A. Klochkov, P.G. Khalatur, A.R. Khokhlov, G. ten Brinke, Microphase separation within a comb copolymer with attractive side chains: A computer simulation study, Macromol. Theory Simul. 10 (2001) 389–394.

[32] A. Yethiraj, A Monte Carlo simulation study of branched polymers, J. Chem. Phys. 125 (2006) 204901, 10 pp.

[33] N.A. Denesyuk, Conformational properties of bottle-brush polymers, Phys. Rev. E 67 (2003) 051803, 10 pp.

[34] S.S. Sheiko, O.V. Borisov, S.A. Prokhorova, M. Möller, Cylindrical molecular brushes under poor solvent conditions: microscopic observation and scaling analysis, Eur. Phys. J. E 13 (2004) 125–131.

[35] S. Elli, F. Ganazzoli, E.G. Timoshenko, Y.A. Kuznetsov, R. Connolly, Size and persistence length of molecular bottle-brushes by Monte Carlo simulations, J. Chem. Phys. 120 (2004) 6257–6267.

[36] R. Connolly, G. Bellesia, E.G. Timoshenko, Y.A. Kuznetsov, S. Elli, F. Ganazzoli, "Intrinsic" and "topological" stiffness in branched polymers, Macromolecules 38 (2005) 5288–5299.

[37] H.-P. Hsu, W. Paul, K. Binder, One- and two-component bottle-brush polymers: Simulations compared to theoretical predictions, Macromol. Theory Simul. 16 (2007) 660–689.

[38] H.-P. Hsu, W. Paul, K. Binder, Simulation of copolymer bottle-brushes, Macromol. Symp. 252 (2007) 58–67.

[39] L.-J. Qu, X. Jin, Q. Liao, Numerical self-consistent field theory of cylindrical polyelectrolyte brushes, Macromol. Theory Simul. 18 (2009) 162–170.

[40] H.-P. Hsu, K. Binder, W. Paul, How to define variation of physical properties normal to an undulating one-dimensional object, Phys. Rev. Lett. 103 (2009) 198301, 4 pp.

[41] H.-P. Hsu, W. Paul, S. Rathgeber, K. Binder, Characteristic length scales and radial monomer density profiles of molecular bottle-brushes: Simulation and experiment, Macromolecules 43 (2010) 1592–1601.

[42] H.-P. Hsu, W. Paul, K. Binder, Standard definitions of persistence length do not describe the local "intrinsic" stiffness of real polymer chains, Macromolecules 43 (2010) 3094–3102.

[43] I. Carmesin, K. Kremer, The bond fluctuation model: A new effective algorithm for the dynamics of polymers in all spatial dimensions, Macromolecules 21 (1988) 2819–2823.

[44] H.P. Deutsch, K. Binder, Interdiffusion and self-diffusion in polymer mixtures: A Monte Carlo study, J. Chem. Phys. 94 (1991) 2294–2304.

[45] W. Paul, K. Binder, D.W. Heermann, K. Kremer, Crossover scaling in semidilute polymer solutions: A Monte Carlo test, J. Phys. II 1 (1991) 37–60.

[46] K. Binder, in: K. Binder (Ed.), Monte Carlo and Molecular Dynamics Simulations in Polymer Science, Oxford Univ. Press, New York, 1995, p. 1.

[47] P. Grassberger, Pruned-enrich Rosenbluth method: Simulations of θ polymers of chain length up to 1 000 000, Phys. Rev. E 56 (1997) 3683–3693.

[48] J.P. Wittmer, P. Beckrich, H. Meyer, A. Cavallo, A. Johner, J. Baschnagel, Intramolecular long-range correlations in polymer melts: The segmental size distribution and its moments, Phys. Rev. E 76 (2007) 011803, 18 pp.

[49] A.D. Sokal, in: K. Binder (Ed.), Monte Carlo and Molecular Dynamics Simulations in Polymer Science, Oxford Univ. Press, New York, 1995, p. 47.

[50] H.-P. Hsu, W. Paul, K. Binder, Conformational studies of bottle-brush polymers absorbed on a flat solid surface, J. Chem. Phys. 133 (2010) 134902, 14 pp.